ChemComm

COMMUNICATION

View Article Online
View Journal | View Issue

Cite this: *Chem. Commun.*, 2021, **57**, 1603

Received 30th October 2020,
Accepted 1st December 2020

DOI: 10.1039/d0cc07199d

rsc.li/chemcomm

Tuning the mechanistic pathways of peptide self-assembly by aromatic interactions†

Goutam Ghosh, * Kalathil K. Kartha and Gustavo Fernández *

Herein, we have unravelled the key influence of aromatic interactions on the mechanistic pathways of peptide self-assembly by introducing suitable chromophores (pyrene *vs.* naphthalene). Although both self-assembled peptides are indistinguishable in their morphologies, this minor structural difference strongly affects the packing modes (parallel *vs.* antiparallel) and the corresponding self-assembly mechanism (cooperative *vs.* isodemsic).

Self-assembly is a ubiquitous phenomenon that regulates key processes and functions in living organisms.[1] Inspired by these sophisticated architectures and with the aim of addressing crucial issues in biology and materials science, a wide variety of artificial building blocks have been explored for constructing programmable self-assembled nanostructures.[2] In this regard, peptides are archetypal building blocks because of their biocompatibility, biodegradability and tunable self-assembly process and corresponding nanostructures.[3] Additionally, experimental variables such as pH, temperature, light, ionic strength, solvent interactions and salt concentration are known to strongly affect the aggregation pathways, mechanism and morphology of peptide assemblies.[4] More importantly, the self-assembly of peptides is largely dominated by the subtle interplay between different attractive non-covalent interactions (such as aromatic, van der Waals, hydrogen bonding (H-bonding) and electrostatic interactions) and repulsive interactions (such as electrostatic interactions among similar charges and steric effects).[5] Among all non-covalent interactions, aromatic interactions not only play a significant role in self-assembly and gelation processes of peptides, but they can also balance the hydrophobicity of the systems.[6] Recently, peptide amphiphiles bearing chromophores such as pyrene,[7a] naphthalene,[7b,c] anthracene,[7d] perylene diimide[7e] and naphthalene diimide[7f] have received considerable attention for the bottom-up construction of tunable luminescent nanomaterials. However, understanding the relationship between aromatic interactions and mechanistic pathways of peptide self-assembly remains elusive.[8]

To address this issue, we herein unravel the role of aromatic interactions on tuning the self-assembly mechanism of peptide assemblies in aqueous media. To demonstrate this approach, we have rationally designed a well-known dipeptide sequence "Phe-Phe" (**FF**)[9] and conjugated it with different π-chromophores such as pyrene (**Py-FF**) and naphthalene (**Nap-FF**) (Scheme 1). Furthermore, a control molecule without chromophore (**Ac-FF**) has also been prepared (Scheme S3 in ESI†). Detailed experimental studies of both peptides unveiled a dramatic change in their mechanistic pathways of supramolecular polymerization (SP) depending on the extent of aromatic interactions (cooperative SP for **Py-FF** *vs.* isodesmic SP for **Nap-FF**). Intriguingly, despite the different assembly mechanism, both molecules self-assemble into the same aggregate morphology (1D nanofibers), which is a rare phenomenon in self-assembly.[10]

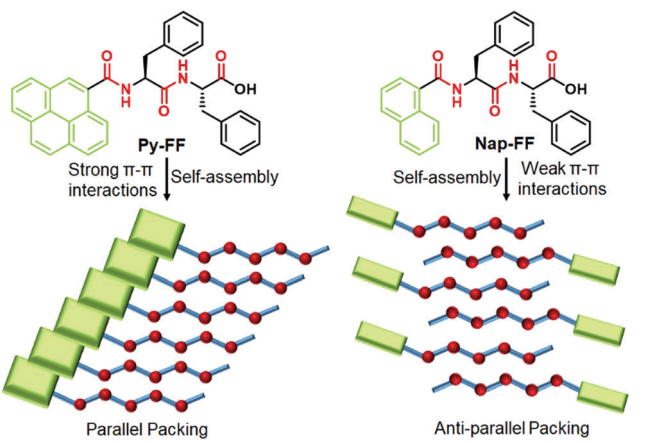

Scheme 1 Chemical structures of **Py-FF** and **Nap-FF** (top) and schematic representation of their packing modes upon aqueous self-assembly (bottom).

Organisch-Chemisches Institut, Westfälische Wilhelms-Universität Münster, Corrensstraße 36, 48149 Münster, Germany. E-mail: gghosh.chem@gmail.com, fernandg@uni-muenster.de

† Electronic supplementary information (ESI) available. See DOI: 10.1039/d0cc07199d

The comparative self-assembly studies of **Py-FF** and **Nap-FF** were investigated by different spectroscopic and microscopic techniques such as UV-vis, fluorescence, circular dichroism (CD), Fourier-transform infrared spectroscopy (FTIR), nuclear magnetic resonance (NMR) and atomic force microscopy (AFM). The UV-vis spectra of **Py-FF** at 1×10^{-4} M and room temperature (RT) in a 'good' solvent such as tetrahydrofuran (THF) shows three sharp bands at 341, 276 and 243 nm (Fig. 1a), indicating a monomeric state.[11] On the other hand, a broad UV-vis spectrum with significant reduction of absorption is observed for **Py-FF** in aqueous media (H_2O/THF = 9/1), suggestive of a plausible self-assembly through strong π–π interactions (Fig. 1a). By contrast, the UV-vis spectra of **Nap-FF** in THF and H_2O (or in H_2O/THF = 9/1) at 1×10^{-4} M and RT exhibit no significant changes, suggesting weak aromatic interactions (Fig. 1e). Fluorescence studies of monomeric **Py-FF** in THF reveal two strong emission bands at 385 and 404 nm that are considerably reduced upon aggregation in H_2O/THF (9/1) (Fig. 1b), suggesting aggregation-caused quenching (ACQ) due to strong π-stacking.[12] This behaviour strongly differs for **Nap-FF** in H_2O, where an enhanced emission intensity was observed compared to THF (Fig. 1f). This behaviour may possibly result from aggregation-induced emission (AIE)[12] owing to weak aromatic interactions between the chromophores, which further corroborates the findings noticed by UV-vis spectroscopy. The significant differences in the strength of aromatic interactions for both peptides are further supported by the observation of up field shifts for the aromatic protons of **Py-FF** in solvent-dependent ^{1}H NMR studies (Fig. S7, ESI†), whereas no such shifts were noticed for **Nap-FF** (Fig. S8, ESI†). FT-IR spectra of both **Py-FF** and **Nap-FF** in THF reveal two sharp peaks at 3569 and 3511 cm^{-1}, corresponding to two different non-hydrogen bonded NH protons (Fig. 1c and g). Notably, these two bands merge into a single band at lower frequency (3410 cm^{-1}) in D_2O, demonstrating the involvement of strong H-bonding. The self-assembly of **Py-FF** and **Nap-FF** was also investigated by CD spectroscopy (Fig. 1d and h). While the solution of monomeric **Py-FF** in THF is nearly CD silent, strong negative CD signals at 340, 285, 242 and 216 nm were observed upon aggregation in H_2O/THF (9/1). The bands at 340, 285 and 242 nm correspond to absorption bands noticed in UV-vis spectroscopy, indicating strong exciton coupling among the pyrene chromophores. The additional intense negative band at 216 nm is suggestive of the formation of β-sheet rich secondary structures. This is further proven by the appearance of two intense peaks at 1634 and 1669 cm^{-1} in the amide I region in FT-IR studies (Fig. S9, ESI†).[13,14] Additionally, a thioflavin T (ThT) assay was also performed to probe β-sheet formation (Fig. S10, ESI†). On the other hand, the CD spectrum of **Nap-FF** in H_2O exhibits an intense single positive band at 222 nm, whereas only residual bands are observed in the region where the naphthalene dye absorbs (250–300 nm; Fig. 1h). These results suggest negligible exciton coupling of the naphthalene chromophores during aqueous self-assembly. The CD signal of **Nap-FF** originates from the **Ac-FF** motif, as a similar positive band at 221 nm arises for the latter in water (Fig. S11, ESI†), suggesting a similar type of orientation. As expected, the nearly CD silent spectrum observed for **Nap-FF** in THF indicates a lack of aggregation in this media (Fig. 1h). Moreover, the CD spectra and ThT assay (Fig. S12, ESI†) of **Nap-FF** rule out the possibility of β-sheet formation, which is further supported by the position of the amide I bands obtained in FT-IR spectra (Fig. S13, ESI†).[14,15] The FT-IR bands of **Ac-FF** (Fig. S14, ESI†) exhibit similar trends as those found for **Nap-FF**, further indicating a similar type of packing. Comparison of the CD spectra and ThT assay of **Py-FF** and **Nap-FF** discloses clear differences in the

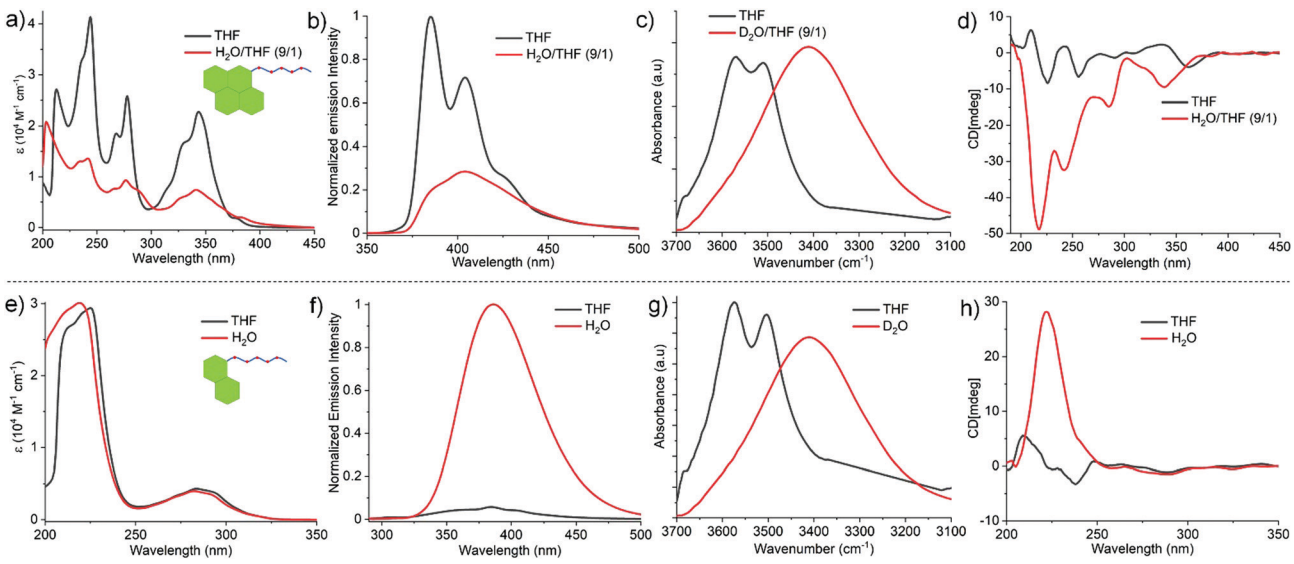

Fig. 1 Solvent-dependent UV-vis spectra of (a) **Py-FF** and (e) **Nap-FF** (the peak below 250 nm corresponds to n–π* band of amides of FF motif); fluorescence spectra of (b) **Py-FF** (excitation wavelength = 340 nm) and (f) **Nap-FF** (excitation wavelength = 290 nm); FTIR spectra of (c) **Py-FF** and (g) **Nap-FF**; CD spectra of (d) **Py-FF** and (h) **Nap-FF** [$C = 1 \times 10^{-4}$ M; T = 298 K].

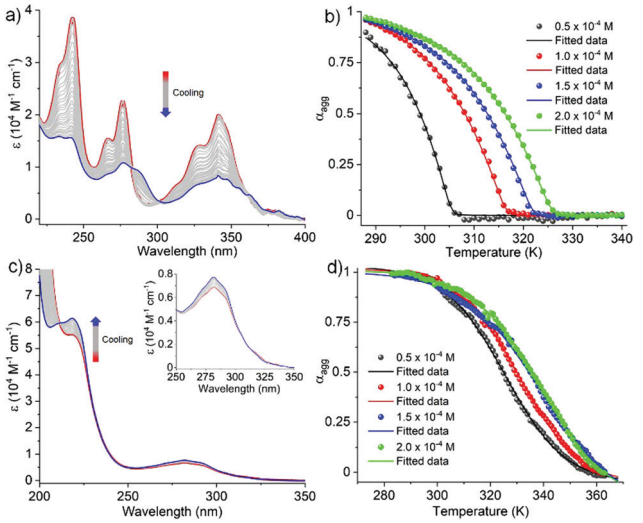

Fig. 2 (a) VT UV-vis spectra of **Py-FF** in H_2O/THF (9/1); (b) cooling curves of **Py-FF** monitored at 243 nm and fitted to the cooperative model; (c) VT UV-vis spectra of **Nap-FF** in H_2O (inset image corresponds to zoomed area of the absorption of naphthalene moiety); (d) cooling curves of **Nap-FF** monitored at 219 nm and fitted to the isodesmic model [cooling rate = 1 K min^{-1}; $C = 1 \times 10^{-4}$ M].

supramolecular organization for both systems,[16] which agrees well with the observations described earlier.

From these observations, we conclude that the self-assembly of **Py-FF** occurs by the synergistic effect of strong π–π interactions between the pyrene motifs and H-bonding involving the peptide groups *via* a parallel molecular organization (Scheme 1). On the other hand, the self-assembly of **Nap-FF** is largely stabilized by H-bonding between the peptide moieties, which have to arrange in a way that no effective aromatic interactions occur between the naphthalene moieties. The arrangement of the **Nap-FF** monomers in an antiparallel fashion, as shown in Scheme 1, might be one plausible possibility that accounts for the experimental observations.

In order to investigate the mechanistic pathways of self-assembly for both **Py-FF** and **Nap-FF** in aqueous media, variable temperature (VT) experiments were carried out by monitoring the UV-vis, fluorescence and CD spectral changes. For **Py-FF**, cooling the solution from 343 to 288 K at a rate of 1 K min^{-1} leads to similar spectral changes to those observed when comparing the UV-vis spectra in THF and aqueous solution (see Fig. 1a), indicating a transition from monomeric to aggregated state (Fig. 2a). The obtained non-sigmoidal cooling curves at different concentrations (Fig. 2b) clearly suggest a cooperative self-assembly pathway driven by synergistic aromatic and intermolecular H-bonding interactions. Global fitting of the cooling curves to the nucleation–elongation (cooperative) model[17] (Fig. 2b) yields the following parameters: $\Delta H^\circ = -64.45$ kJ mol^{-1}, $\Delta S^\circ = -127.31$ J mol^{-1} K^{-1}, $\Delta G^\circ = -26.49$ kJ mol^{-1} and degree of cooperativity (σ) = 4.5×10^{-5} (Table 1). The cooperative mechanism was also supported by the non-sigmoidal cooling curves extracted from VT-CD (Fig. S16, ESI†) and VT-fluorescence studies (Fig. S17, ESI†).

In contrast to **Py-FF**, VT-UV-vis cooling experiments for **Nap-FF** (from 363 to 283 K; 1 K min^{-1}) disclose clear sigmoidal curves at different concentrations (Fig. 2d), indicating an isodesmic supramolecular polymerization.[18] This switch in mechanism from cooperative (for **Py-FF**) to isodesmic (for **Nap-FF**) can be rationalized by the lack of synergistic non-covalent interactions for the latter, *i.e.* largely driven by intermolecular H-bonding.[19] Application of the isodesmic model to the experimental data allows the derivation of the corresponding thermodynamic parameters (Fig. S19, ESI†): $\Delta H = -74.19$ kJ mol^{-1}, $\Delta S = -151.31$ J mol^{-1} K^{-1}, $\Delta G^\circ = -29.1$ kJ mol^{-1} (Table 1). In analogy to **Py-FF**, the isodesmic mechanism for **Nap-FF** was further supported by VT-CD (Fig. S20, ESI†) and VT-fluorescence studies (Fig. S21, ESI†).

Interestingly, in stark contrast to most examples of supramolecular assemblies reported to date, the different assembly mechanism for **Py-FF** and **Nap-FF** is not accompanied by a significant change in aggregate morphology. Microscopic studies by AFM on mica disclose similar type of fiber-like 1D morphologies for both compounds. Whereas **Py-FF** self-assembles into 1D nanofibers (height 2.5 ± 0.3 nm and width 60-70 nm) with lengths of several micrometers (Fig. 3a and Fig. S22, ESI†), bundled 1D nanofibers (Fig. 3b; height 3.0 ± 0.5 nm and width 35 nm of single fiber, Fig. S23, ESI†) are formed by **Nap-FF**. The higher tendency of **Nap-FF** to bundle might be explained by the difficulty in shielding the hydrophobic naphthalene core from the polar solvent molecules in the proposed antiparallel arrangement (see Scheme 1), leading to a more pronounced lateral growth.

In summary, we have rationally designed two peptide amphiphiles with different chromophores (pyrene: **Py-FF** and naphthalene: **Nap-FF**) and studied their comparative aqueous self-assembly by various techniques. Interestingly, the different extent of aromatic interactions of the pyrene and naphthalene groups governs the packing modes (parallel for **Py-FF** *vs.* antiparallel for **Nap-FF**) and the resulting self-assembly mechanism (cooperative for **Py-FF** *vs.* isodesmic for **Nap-FF**). Despite these marked differences, both molecules form the same type of aggregate morphology (1D nanofibers), a phenomenon that is

Table 1 Thermodynamic parameters obtained from temperature-dependent UV-vis experiments of **Py-FF** and **Nap-FF**

Compound	ΔH° [kJ mol^{-1}]	ΔS° [J mol^{-1} K^{-1}]	ΔH°_{nucl} [kJ mol^{-1}]	T_e/K	ΔG° [kJ mol^{-1}]	K_{el}/M^{-1} [298 K]	K_{nucl}/M^{-1} [298 K]	σ
Py-FF	−64.45	−127.31	−24.81	316.1	−26.49	4.4×10^4	1.98	4.5×10^{-5}

	ΔH [kJ mol^{-1}]	ΔS [J mol^{-1} K^{-1}]	ΔG° [kJ mol^{-1}]	K_a/M^{-1} [298 K]
Nap-FF	−74.19	−151.31	−29.10	1.7×10^5

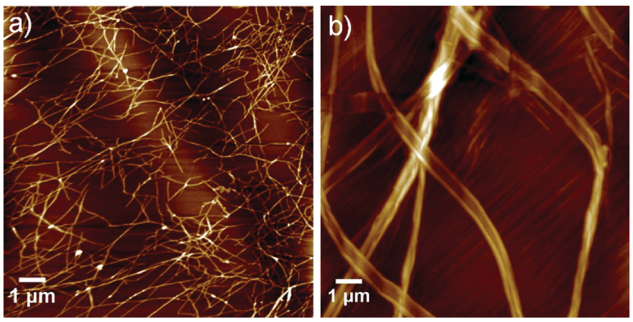

Fig. 3 AFM images of (a) **Py-FF** and (b) **Nap-FF** [$C = 1 \times 10^{-4}$ M].

rare in self-assembly. Our experimental findings highlight the importance of aromatic interactions in controlling the mechanism of peptide self-assembly and, consequently, the properties of the secondary structures, which may have important implications in the biomedical field.

G. G., K. K. K. and G. F. thank the European Commission (European Research Council) for funding (ERC-StG-2016 SUPRACOP-715923).

Conflicts of interest

There are no conflicts to declare.

Notes and references

1 G. M. Whitesides, J. P. Mathias and C. T. Seto, *Science*, 1991, **254**, 1312.
2 (*a*) T. Aida, E. W. Meijer and S. Stupp, *Science*, 2012, **335**, 813; (*b*) C. Rest, R. Kandanelli and G. Fernández, *Chem. Soc. Rev.*, 2015, **44**, 2543; (*c*) Z. Chen, A. Lohr, C. R. Saha-Möller and F. Würthner, *Chem. Soc. Rev.*, 2009, **38**, 564; (*d*) S. S. Babu, V. K. Praveen and A. Ajayaghosh, *Chem. Rev.*, 2014, **114**, 1973; (*e*) G. Ghosh, P. Dey and S. Ghosh, *Chem. Commun.*, 2020, **56**, 6757.
3 (*a*) F. Qiu, Y. Chen, C. Tang and X. Zhao, *Int. J. Nanomed.*, 2018, **13**, 5003; (*b*) W. K. Restu, Y. Nishida, S. Yamamoto, J. Ishii and T. Maruyama, *Langmuir*, 2018, **34**, 8065; (*c*) E. Radvar and H. S. Azevedo, *Macromol. Biosci.*, 2019, **19**, 1800221; (*d*) D. E. Clarke, C. D. J. Parmenter and O. A. Scherman, *Angew. Chem., Int. Ed.*, 2018, **57**, 7709; (*e*) Q. Meng, Y. Kou, X. Ma, Y. Liang, L. Guo, C. Ni and K. Liu, *Langmuir*, 2012, **28**, 5017.
4 (*a*) G. Ghosh, R. Barman, J. Sarkar and S. Ghosh, *J. Phys. Chem. B*, 2019, **123**, 5909; (*b*) G. Ghosh and G. Fernández, *Beilstein J. Org. Chem.*, 2020, **16**, 2017; (*c*) H. Frisch, Y. Nie, S. Raunser and P. Besenius, *Chem. – Eur. J.*, 2015, **21**, 3304; (*d*) K. Bauri, M. Nandi and P. De, *Polym. Chem.*, 2018, **9**, 1257; (*e*) N. Falcone and H. B. Kraatz, *Chem. – Eur. J.*, 2018, **24**, 14316; (*f*) P. A. Korevaar, C. J. Newcomb, E. W. Meijer and S. I. Stupp, *J. Am. Chem. Soc.*, 2014, **136**, 8540; (*g*) D. Spitzer, L. L. Rodrigues, D. Straßburger, M. Mezger and P. Besenius, *Angew. Chem., Int. Ed.*, 2017, **56**, 15461.
5 (*a*) J. Wang, K. Liu, R. Xing and X. Yan, *Chem. Soc. Rev.*, 2016, **45**, 5589; (*b*) R. Otter and P. Besenius, *Org. Biomol. Chem.*, 2019, **17**, 6719.
6 (*a*) A. Dasgupta and D. Das, *Langmuir*, 2019, **35**, 10704; (*b*) S. Fleming and R. V. Ulijn, *Chem. Soc. Rev.*, 2014, **43**, 8150; (*c*) A. Ustinov, H. Weissman, E. Shirman, I. Pinkas, X. Zuo and B. Rybtchinski, *J. Am. Chem. Soc.*, 2011, **133**, 16201.
7 (*a*) B. Pramanik, N. Singha and D. Das, *ACS Appl. Polym. Mater.*, 2019, **1**, 833; (*b*) L. Chen, K. Morris, A. Laybourn, D. Elias, M. R. Hicks, A. Rodger, L. Serpell and D. J. Adams, *Langmuir*, 2010, **26**, 5232; (*c*) A. Das and S. Ghosh, *Chem. – Eur. J.*, 2010, **16**, 13622; (*d*) P. K. Gavel, D. Dev, H. S. Parmar, S. Bhasin and A. K. Das, *ACS Appl. Mater. Interfaces*, 2018, **10**, 10729; (*e*) S. Ahmed, K. N. Amba Sankar, B. Pramanik, K. Mohanta and D. Das, *Langmuir*, 2018, **34**, 8355; (*f*) N. Singha, P. Gupta, B. Pramanik, S. Ahmed, A. Dasgupta, A. Ukil and D. Das, *Biomacromolecules*, 2017, **18**, 3630.
8 S. Ogi, K. Matsumoto and S. Yamaguchi, *Angew. Chem., Int. Ed.*, 2018, **57**, 2339.
9 (*a*) M. Reches and E. Gazit, *Science*, 2003, **300**, 625; (*b*) S. Marchesan, A. V. Vargiu and K. E. Styan, *Molecules*, 2015, **20**, 19775.
10 N. M. Casellas, S. Pujals, D. Bochicchio, G. M. Pavan, T. Torres, L. Albertazzi and M. García-Iglesias, *Chem. Commun.*, 2018, **54**, 4112.
11 J. Duhamel, *Polymers*, 2012, **4**, 211.
12 (*a*) F. Würthner, *Angew. Chem., Int. Ed.*, 2020, **59**, 14192; (*b*) Z. Zhao, H. Zhang, J. W. Y. Lam and B. Z. Tang, *Angew. Chem., Int. Ed.*, 2020, **59**, 9888.
13 (*a*) P. I. Haris and D. Chapman, *Biopolymers*, 1995, **37**, 251; (*b*) M. Jackson and H. H. Mantsch, *Crit. Rev. Biochem. Mol. Biol.*, 1995, **30**, 95; (*c*) J. P. Schneider, D. J. Pochan, B. Ozbas, K. Rajagopal, L. Pakstis and J. Kretsinger, *J. Am. Chem. Soc.*, 2002, **124**, 15030; (*d*) H. Yan, A. Saiani, J. E. Gough and A. F. Miller, *Biomacromolecules*, 2006, **7**, 2776.
14 (*a*) N. Yamada, K. Ariga, M. Naito, K. Matsubara and E. Koyama, *J. Am. Chem. Soc.*, 1998, **120**, 12192; (*b*) Y. Zou, Y. Li, W. Hao, X. Hu and G. Ma, *J. Phys. Chem. B*, 2013, **117**, 4003.
15 The absence of amide I bands below 1640 cm^{-1} and above 1680 cm^{-1} for **Nap-FF** supports its inability to form antiparallel β-sheets (for details, see ref. 14).
16 (*a*) Y. Zhang, H. Gu, Z. Yang and B. Xu, *J. Am. Chem. Soc.*, 2003, **125**, 13680; (*b*) P. G. Argudo, R. Contreras-Montoya, L. Á. de Cienfuegos, J. M. Cuerva, M. Cano, D. Alba-Molina, M. T. Martín-Romero, L. Camacho and J. J. Giner-Casares, *Soft Matter*, 2018, **14**, 9343.
17 (*a*) H. M. M. ten Eikelder, A. J. Markvoort, T. F. A. de Greef and P. A. J. Hilbers, *J. Phys. Chem. B*, 2012, **116**, 5291; (*b*) A. J. Markvoort, H. M. M. ten Eikelder, P. A. J. Hilbers, T. F. A. de Greef and E. W. Meijer, *Nat. Commun.*, 2011, **2**, 509.
18 M. M. J. Smulders, M. M. L. Nieuwenhuizen, T. F. A. de Greef, P. van der Schoot, A. P. H. J. Schenning and E. W. Meijer, *Chem. – Eur. J.*, 2010, **16**, 362.
19 (*a*) M. M. L. Nieuwenhuizen, T. F. A. de Greef, R. L. J. van der Bruggen, J. M. J. Paulusse, W. P. J. Appel, M. M. J. Smulders, R. P. Sijbesma and E. W. Meijer, *Chem. – Eur. J.*, 2010, **16**, 1601; (*b*) W. P. J. Appel, M. M. L. Nieuwenhuizen and E. W. Meijer, in *Supramolecular Polymer Chemistry*, ed. A. Harada, Wiley-VCH, Germany, 2012, ch. 1, vol. 1, pp. 1–28.